

P10R.4 VALIDATION OF FIRST GENERATION CASA RADARS WITH CSU-CHILL

Francesc Junyent¹, V. Chandrasekar², D. Brunkow², P.C. Kennedy², D.J. McLaughlin¹
¹ University of Massachusetts, Amherst, Massachusetts
² Colorado State University, Fort Collins, Colorado

1. INTRODUCTION

The National Science Foundation Engineering Research Center for Collaborative Adaptive Sensing of the Atmosphere (CASA) [McLaughlin et al., 2005] will be deploying the first generation of an automated network of four low-power, X-band, polarimetric, Doppler radars in Oklahoma in spring 2006. This radar network, known as NETRAD, will map precipitation and detect, locate and track severe weather events such as tornadoes through coordinated interaction of all its radar nodes via a real-time, closed-loop control system. A prototype of the sensing node has been completed, and was deployed for the first time in Colorado side-by-side with the Colorado State University's CHILL radar (S-band). During three weeks of operation the CASA NETRAD sensing node prototype, referred to as MA-1, underwent experiments to calibrate and characterize the performance of different system components. MA-1 also scanned through two different weather events simultaneously with CHILL, generating a co-located and synchronized data set at both X-band and S-band. The S-band data set was used as a comparison benchmark. This paper will present the CASA NETRAD sensing node calibration results, and a comparison of the results obtained at X-band and S-band for the simultaneously scanned weather events.

2. MA-1 AND CHILL RADAR DESCRIPTIONS

The CASA NETRAD sensing node prototype [Junyent et al., 2005], MA-1, is built around a low-power magnetron transmitter, with low-cost and small physical size driving the design while meeting stringent specifications. The transmitter and dual-channel receiver are packaged together in a compartmented box above both axes of motion, attached behind the dual-polarization center-fed reflector antenna. A linear actuator moves this ensemble in elevation, while an agile

pedestal creates the motion in azimuth. The radar echoes are fed into a reconfigurable data acquisition and processing system newly developed as part of the radar node [Khasgiwale et al., 2005], which also generates the transmitter trigger and receiver control waveforms. The whole radar assembly is housed inside a 2.4 m diameter 2.4 m height fiber radome, and is remotely operated via Ethernet. Table 1 shows some of MA-1 relevant characteristics.

Table 1. MA-1 specifications

Frequency	9431 ± 30 MHz
Maximum Peak Power	25 kW
Maximum Duty Cycle	0.2 %
Maximum Pulse length	2 μs
Tx Polarization	Elliptical (Hybrid mode)
Rx Polarization	Dual linear V and H
Rx gain	30 dB
Final Dynamic Range referenced at input (BW = 1.5 MHz)	-106.2 dBm to -3 dBm
Antenna diameter	1.2 m
Antenna Gain	38 dB
Antenna Beamwidth	1.8 deg

The CSU-CHILL radar [Brunkow et al., 2000] consists of a high-power klystron based dual transmitter, and a set of dual, parallel receivers (high gain, and low gain) to increase the system's final dynamic range. The transmitter and receiver systems are housed in a semi trailer, from which two waveguide runs transport the signals to and from the antenna feed point. The antenna and pedestal are protected by an air-inflated radome with an equatorial diameter of 22.3 m and a maximum height of 16.2 m. CHILL is controlled remotely and can be operated over the internet via the VCHILL system. Some of CHILL's main characteristics are shown in Table 2.

In order to be deployed next to CHILL, MA-1 was mounted on a flat-bed truck and driven from Massachusetts to Colorado, where it was finally parked alongside CHILL as shown in Figure 1.

^{*}Corresponding author address: Francesc Junyent, University of Massachusetts, Electrical and Computer Engineering, Amherst, MA 01003; e-mail: junyent@mirsl.ecs.umass.edu

Table 2. CHILL specifications

Frequency	2725 MHz
Maximum Peak Power	1 MW
Maximum PRF	1.25 KHz
Maximum Pulse length	1 μ s
Tx Polarization	Elliptical (Hybrid mode)
Rx Polarization	Dual linear V and H
Final Dynamic Range referenced at input (BW = 0.75 MHz)	96 dB
Antenna diameter	8.5 m
Antenna Gain	43 dB
Antenna Beamwidth	1.1 deg



Figure 1. CHILL (left of image) and truck-mounted MA-1 deployed side-by-side in the CSU-CHILL radar facility, scanning through a convective storm.

3. DEPLOYMENTS AND COLLECTED DATA COMPARISON

Once MA-1 was operational in the deployment site, a number of calibration experiments were conducted to assess and ensure its performance.

To allow coordinated scanning with CHILL, the truck platform was leveled and solar observations were used to find an absolute reference point for azimuth and elevation scanning. Figure 2 shows how the sun observed position was determined from the radar receiver noise-floor fluctuation.

The MA-1 radar receiver was tested, and a combination of various single tone and noise-source measurements were made to check gain differences and drifts between its channels, as well as the overall analog system gain. These measurements were used to determine the

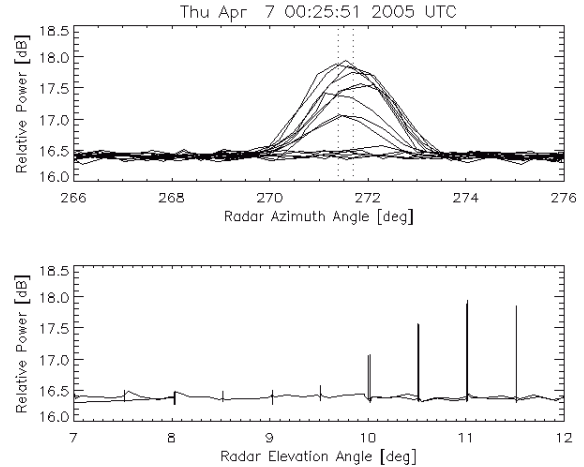
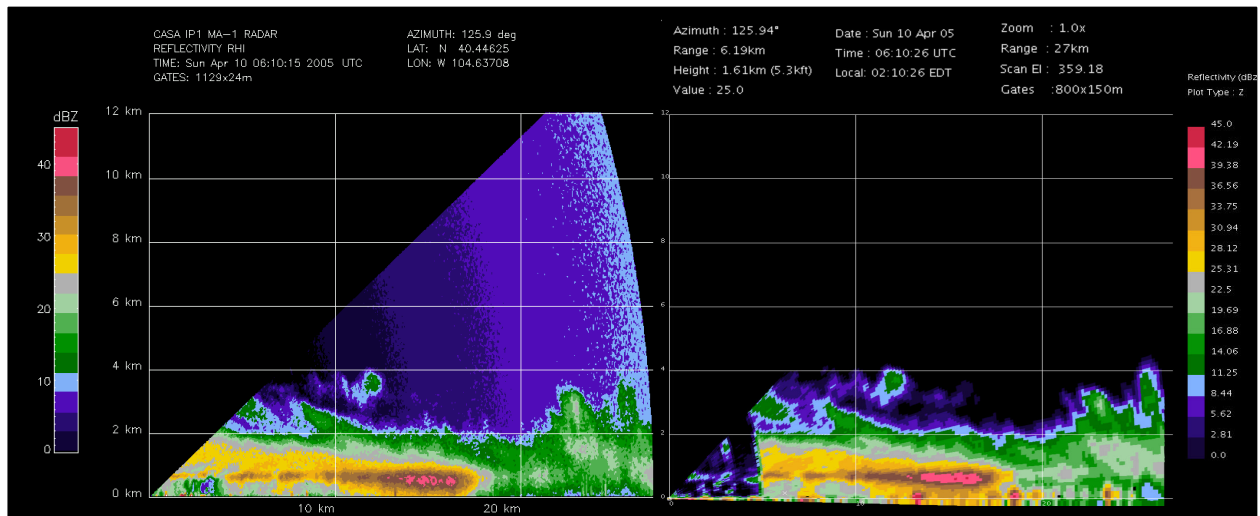


Figure 2. MA-1 horizontal polarization noise floor power fluctuations scanning around the sun.

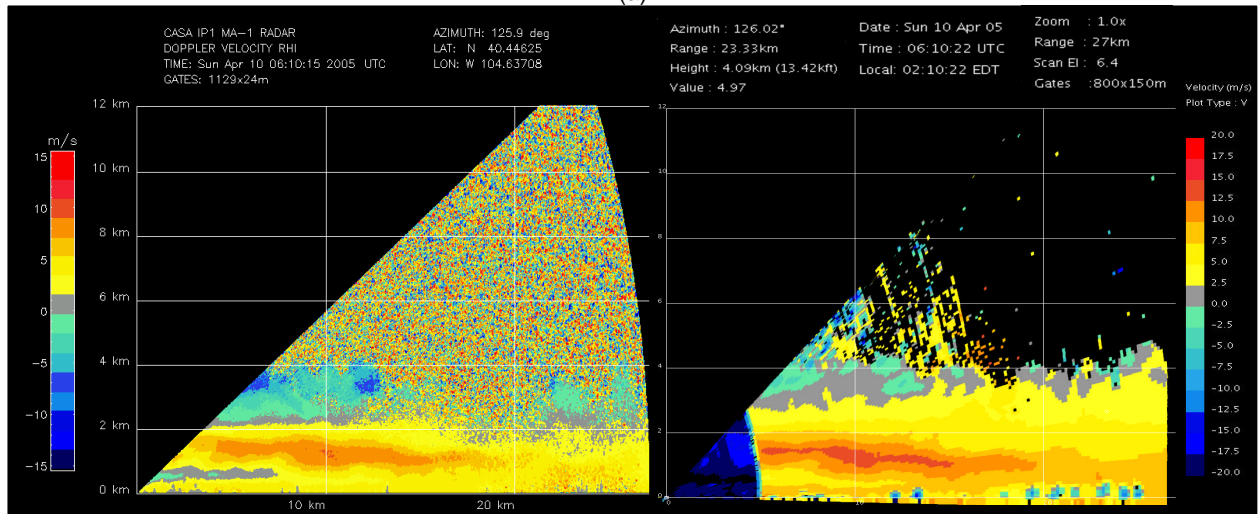
radar constant, together with solar observations and a metallic sphere calibration.

MA-1 and CHILL simultaneously collected data in a variety of scanning modes (RHI, PPI, sector, and fixed angle) during two weather events. Figure 3 shows images from a winter storm on 10 April 2005. Reflectivity shows a band of increasing values, corresponding to snow, at an altitude around 700 m, extending out to 17 km in range and reaching the ground after 10 km. The maximum reflectivity values observed are around 40 dBZ, and both MA-1 and CHILL images reveal the same features and details with little or no difference. The Doppler velocity field is almost uniformly descending, with increasing velocities above the area corresponding to the highest reflectivity. The color discrepancy between the CHILL and MA-1 images is due to different unambiguous Doppler intervals. Cross-correlation coefficient shows a band of lower values corresponding to the bright band in both images, due to the decorrelation effect of melting snow. The low cross-correlation values at the MA-1 farther ranges are caused by limited SNR.

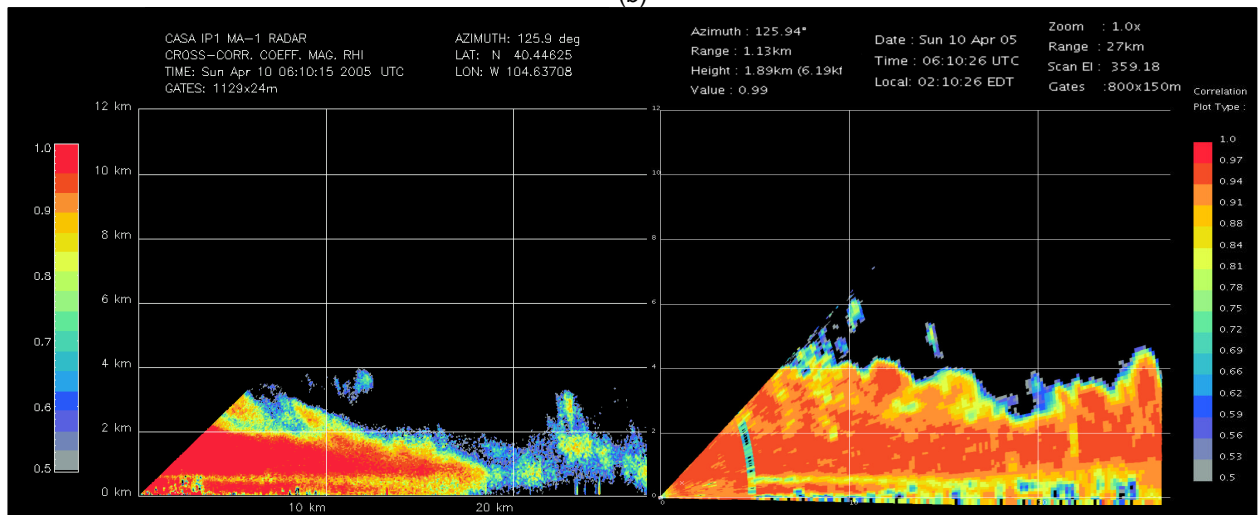
Figure 4 shows data collected during a convective storm on 19 April 2005. In both MA-1 and CHILL reflectivity shows a towering structure with values around 50 dBZ extending out to 15 km in range. After that, the combined effect of attenuation and higher minimum detectable signal of MA-1 make the images differ. On the other hand, the Doppler velocity measurements show a very similar structure for both radars, with the main differences between both images being due to velocity folding and limited SNR zones in the MA-1 measurement. Again, the color discrepancy



(a)

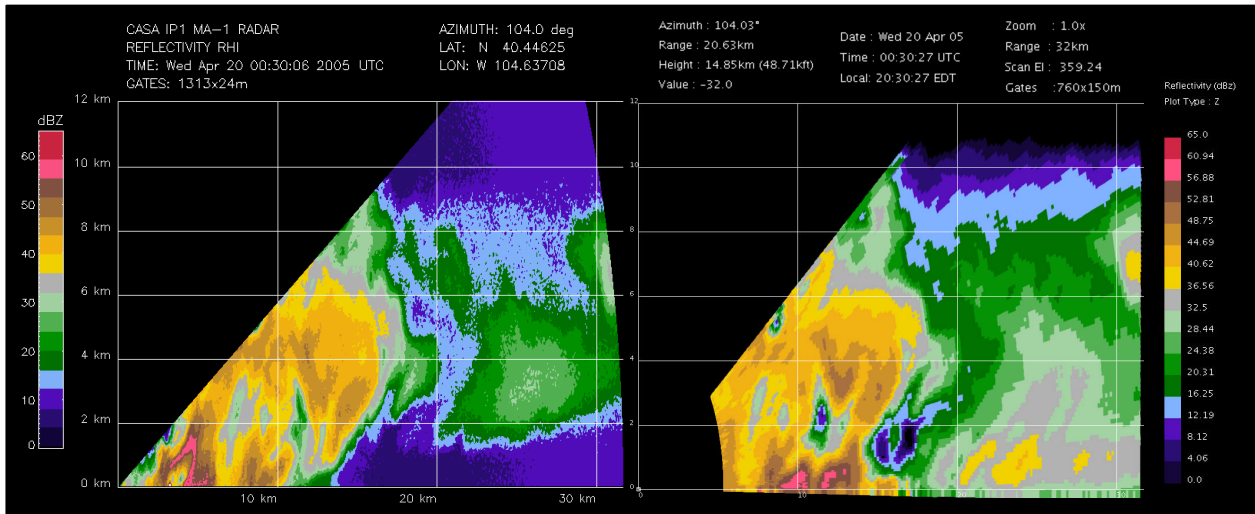


(b)

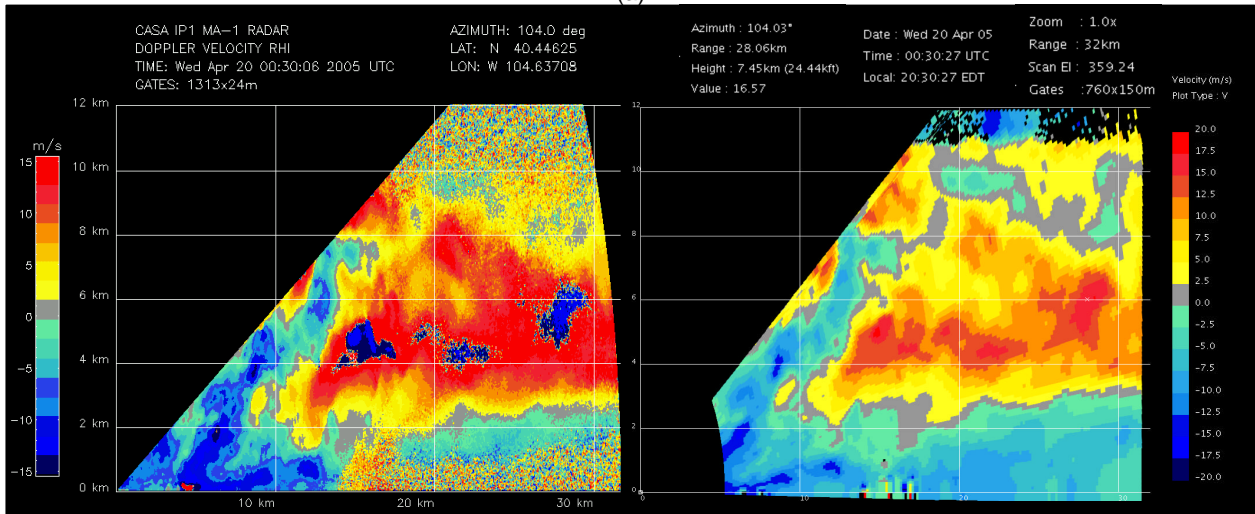


(c)

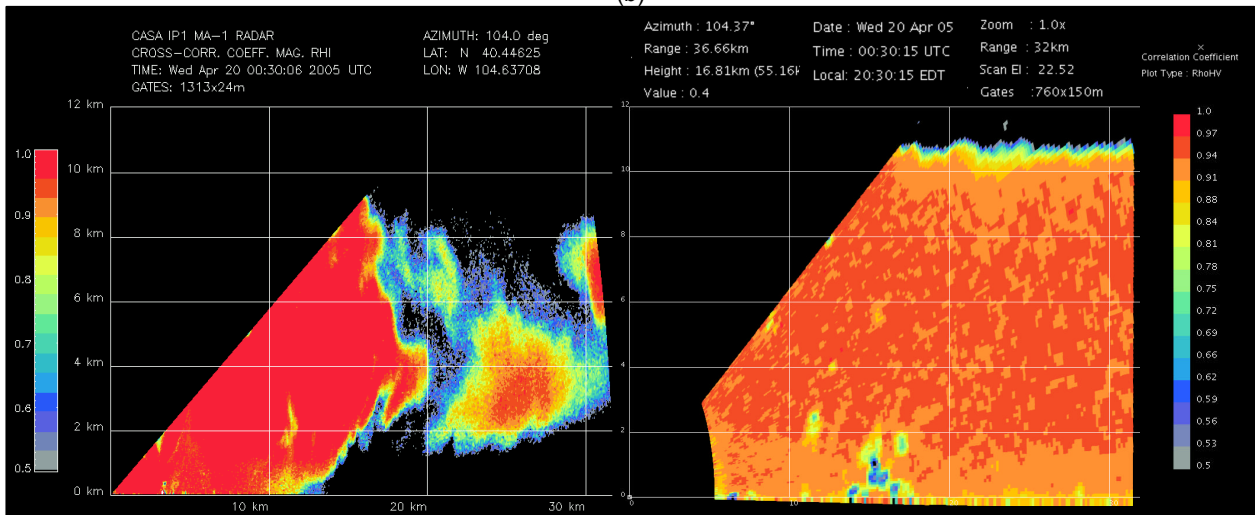
Figure 3. (a) Reflectivity, (b) Doppler velocity, and (c) cross-correlation coefficient RHI plots through a winter storm on 10 April 2005. Left of image is MA-1 and right is CHILL data



(a)



(b)



(c)

Figure 4. (a) Reflectivity, (b) Doppler velocity, and (c) cross-correlation coefficient RHI plots through a convective storm on 19 April 2005. Left of image is MA-1 and right is CHILL data

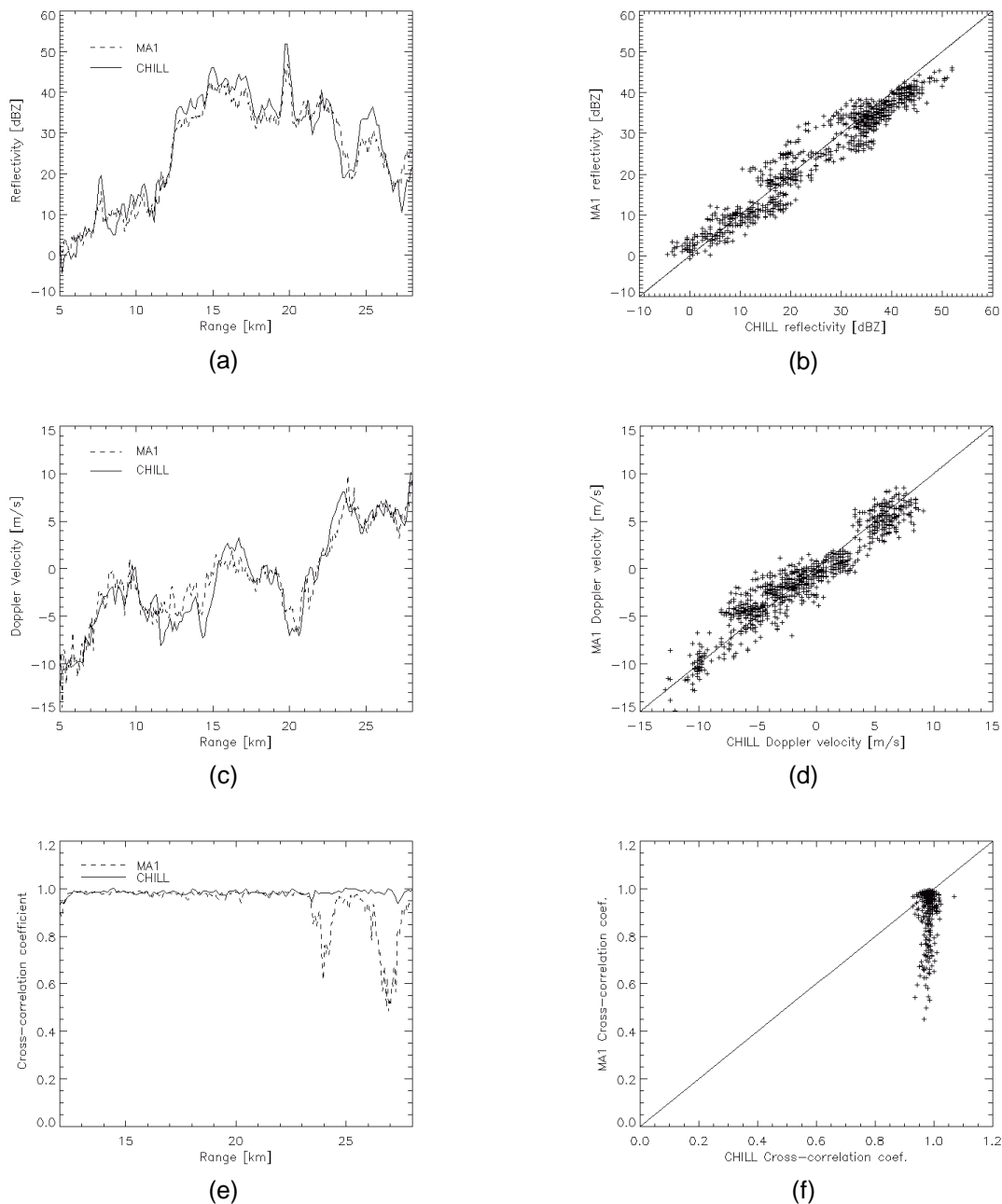


Figure 5. CHILL and MA-1 reflectivity (a) range profiles, and (b) scatter plot. Doppler velocity (c) range profiles, and (d) scatter plot. Cross-correlation coefficient (e) range profiles, and (f) scatter plot.

between the CHILL and MA-1 images is due to different unambiguous Doppler intervals. As in the previous case, cross-correlation coefficient values agree in the high SNR zones only.

To perform a more detailed comparison between the two radars, a data set collected at a fixed angle (not scanning), through the same convective event is used. Reflectivity, Doppler

velocity, and cross-correlation coefficient as a function of range for both radars are shown in Figure 5 (a), (c), (e), demonstrating good agreement. The two radar measurements are then used to create scatter plots. The reflectivity scatter plot, Figure 5 (b), shows how the lower reflectivity values are biased towards MA-1 due to its higher minimum detectable level, and the

higher reflectivity values are biased towards CHILL probably due to the higher attenuation experienced by MA-1. The Doppler velocity scatter plot in Figure 5 (d), does not reveal any significant bias between the two measurements. Cross-correlation coefficient is in good agreement for the high SNR points, with the scatter plot in Figure 5 (f) showing how most of the occurrences fall around the expected (1,1) coordinate. The farther range SNR limited MA-1 measurements create the vertical dispersion in the scatter plot.

In all cases, some of the dispersion between MA-1 and CHILL measurements could be explained by the difference in antenna beam width, as well as some remaining inaccuracy in the relative positioning of both radar beams.

4. CONCLUSIONS

The comparison between simultaneous data sets of the CASA NETRAD radar prototype, MA-1, against CSU-CHILL do not reveal any significant artifact or systematic difference between the two, except those due to attenuation and higher minimum detectable signal in MA-1, which were expected. This experiment validates the CASA NETRAD radar design and operation as a system, and construction of subsequent units is pursued.

5. ACKNOWLEDGEMENTS

Mr. L. Krnan, Mr. R. Ahmed and Dr. M. Zink from the University of Massachusetts and Mr. R.

Bowie from Colorado State University provided support during the deployment.

This work was supported primarily by the Engineering Research Centers Program of the National Science Foundation under NSF Award Number 0313747.

6. REFERENCES

Brunkow, D. et al., 2000: A description of the CSU-CHILL National Radar Facility, *J. of Atmospheric and Oceanic Technology*, **17**, 1596-1608

Khasgiwale, R. et al., 2005: Reconfigurable data acquisition system for weather radar applications, in *Proc. of International Midwest Symposium on Circuits and Systems, Cincinnati, Ohio*.

Junyent, F. et al., 2005: Salient features of radar nodes of the first generation NETRAD system, in *Proc. of International Geoscience and Remote Sensing Symposium, Seoul, Korea*.

McLaughlin, D. J. et al., 2005: Distributed Collaborative Adaptive Sensing (DCAS) for improved detection, understanding, and predicting of Atmospheric hazards, in *Proc. of 85th AMS Annual Meeting, San Diego, California*.